Vol 18 No 10, October 2009
1674-1056/2009/18(10)/4251–08

Chinese Physics B

© 2009 Chin. Phys. Soc.
and IOP Publishing Ltd

Investigation of odd-parity Rydberg states of Eu I with autoionization detection*

Xiao Ying(肖 颖), Dai Chang-Jian(戴长建)†, and Qin Wen-Jie(秦文杰)

Key Laboratory of Display Materials and Photoelectric Devices, Ministry of Education, Tianjin 300191, *China*

School of Science, Tianjin University of Technology, Tianjin 300384, *China*

(Received 2 January 2009; revised manuscript received 11 March 2009)

Isolated-core-excitation (ICE) scheme and autoionization detection are employed to study the bound Rydberg states of europium atom. The high-lying states with odd parity have been measured using the autoionization detection method with three different excitation paths via $4f^7 6s6p[^8P_{5/2}]$, $4f^7 6s6p[^8P_{7/2}]$ and $4f^7 6s6p[^8P_{9/2}]$ intermediate states, respectively. In this paper the spectra of bound Rydberg states of Eu atom are reported, which cover the energy regions from 36000 cm^{-1} to 38250 cm^{-1} and from 38900 cm^{-1} to 39500 cm^{-1}. The study provides the information about level energy, the possible J values and relative line intensity as well as the effective principal quantum number n^* for these states. This work not only confirms the previous results of many states, but also discovers 11 new Rydberg states of Eu atom.

Keywords: europium atom, isolated-core-excitation, bound Rydberg state, autoionization detection

PACC: 3280, 3270

1. Introduction

The study of atomic Rydberg levels has recently received much attention, due to its close relationship with many interesting phenomena, such as propagation without absorption[1] and coherent control,[2] etc. Furthermore, it was also listed as an important candidate for lasing without population inversion.[3]

In spite of numerous applications, the information about the highly excited states of the rare-earth atoms[4–6] is still scanty. Especially, only few studies on the Eu atom have been reported.[7] Among the rare-earth atoms, the Yb atom has been studied most[8,9] due to the fact that the $4f$ shell is completely filled. With only two s-electrons outside the closed shell, the spectrum of the Yb atom is basically an alkaline-earth-like one. However, with a half-filled $4f$ shell, the Eu atom is very active and thus has a much more complex nature in its spectra. Therefore, only few studies on Eu atom have been reported. Although some works on the Eu atom have been done, they only reported odd-parity states[10] in the energy region 45000 cm^{-1}–45735 cm^{-1} and autoionization states[11] using two-step laser photoionization.

Based on the above facts, it is apparent that the study of the highly excited states of the Eu atom is very necessary and challenging. In this work, there are several differences from the earliar reports: a) the ICE scheme and autoionization detection are combined to measure the Rydberg states of the Eu atom; b) the spectra of the 36000 cm^{-1}–38250 cm^{-1} and 38900 cm^{-1}–39500 cm^{-1} energy regions are measured; c) the observations are carried out through three different excitation paths via $4f^7 6s6p[^8P_{5/2}]$, $4f^7 6s6p[^8P_{7/2}]$ and $4f^7 6s6p[^8P_{9/2}]$ intermediate states, respectively.

It is well known that the ICE scheme has been used not only for the study of autoionization spectra of the Ba atom,[12–15] but also for the detection of the Rydberg levels of alkaline-earth atoms.[16–18] However, it has not been utilized for studying the more complex such as the Eu atom. Due to the fact that the autoionization process has many attractive advantages over direct photoionization, this work will systemically measure the spectra of odd-parity Rydberg states of Eu atom with the combining ICE scheme and the autoionization detection. In order to demonstrate that autoionization detection can

*Project supported by the National Natural Science Foundation of China (Grant Nos 10574098, 10674102) and the Natural Science Foundation of Tianjin (Grant No 05YFJMJC05200).

†Corresponding author. E-mail: cjdai@yahoo.com.cn

be much more efficient and selective than the traditional detection methods for detecting Rydberg levels of complex atoms, the Rydberg atoms are driven to the autoionizing states and detected via an autoionization process. Furthermore, the study of the Eu $6snl$ (l=0, 2) Rydberg states with autoionization detection will also prove that it is very versatile in detecting both the low- and high-lying members of a Rydberg series.

With a detailed analysis on the spectral data, we not only identify lots of odd-parity states of Eu atom, but also enrich the database by adding more information which cannot be found in the literatures, such as the possible J value and intensity of the Rydberg states. In the following, an introduction of the experiment will be given in Section 2; the experimental results and discussion are presented in Section 3, and Section 4 gives main conclusions.

2. Experiment

The experimental setup used here is shown in Fig.1. It consists of three parts: a laser system, a vacuum chamber and a data acquisition system. All the lasers used in the experiments are manufactured by quanta system: a giant-770 model Nd:YAG pulsed laser with pulse width 6–8 ns running at 20 Hz; three D-100 model dye lasers with line-width 0.1 cm^{-1}. The first and third dye lasers are pumped by the third harmonic of the Nd:YAG laser and the second one is pumped by the second harmonic of the Nd:YAG laser. The Eu atom source is from an effusive atomic beam sprayed from a resistively heated oven in a vacuum chamber. The atomic beam is collimated and directed to a region between two electric field plates, 1 cm apart, where it is crossed perpendicularly by the three laser beams to avoid the Doppler broadening. The data acquisition system including a model 4121B Boxcar and a 9650A digital pulse generator which are controlled by a computer is from AMETEC Company. In order to ensure the excitation sequence the second and third laser pulses are delayed by 8–10 ns and 16–20 ns respectively with respect to that of the first laser, while the gate of Boxcar and the pulse of electric field are also carefully controlled. Namely, about 0.5 μs after the laser pulses, the ions, resulting from the excitation and subsequent decay of autoionizing states, are extracted by the pulsed electric field to an MCP detector, the output of which is fed into the Boxcar and stored in a computer for further analysis.

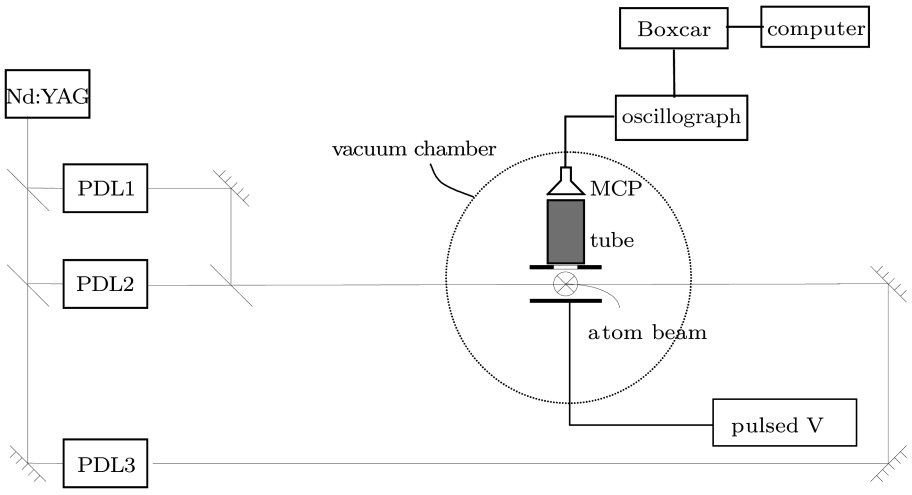


Fig.1. The schematic diagram of the experimental apparatus. It includes the excitation lasers (PDL: pulsed dye laser), the atomic beam, and the detection-analysis systems. The atomic beam is produced in the vacuum chamber, while the ions are detected by an MCP whose signals are averaged by a Boxcar, and stored in a computer for further analysis.

Figure 2 shows the energy-level diagram and the ICE scheme for the Eu atom Rydberg states. With the ICE scheme, the Eu atom is excited from the ground state $4f^76s^2$ to a $4f^76s6p$ state by the first dye laser. Then the atom is excited to a $4f^76snl$ (l=0, 2) Rydberg state, whose outer nl (l=0, 2) electron is in an orbit with a large radius far from the Eu$^+$ $4f^76s$ core, by the second tunable dye laser.

Finally, the atom is excited to an autoionizing state with the transition $6s^+ \rightarrow 6p^+$ by the third dye laser, avoiding the interference from the excitation of the nl electron. Due to considerable interaction with underlying continua converging to the $4f^7 6s^+$ or $4f^7 5d^+$ ionization limit, the atom in the $4f^7 6pnl$ (l=0, 2) autoionizing state is very unstable, and decays quickly into an ion and an electron to a certain ionic state ($4f^7 6s^+$ or $4f^7 5d^+$).

As the autoionization detection, in which the Rydberg atom is driven to the autoionizing state and detected via an autoionization process, can be much more efficient and selective than the traditional detection methods, it is used to detect bound Rydberg states of the Eu stom. To our knowledge, this is the first attempt for this complex atom. Furthermore, the three-step and three-color resonance ionization schemes are applied for three different paths, as described bellow:

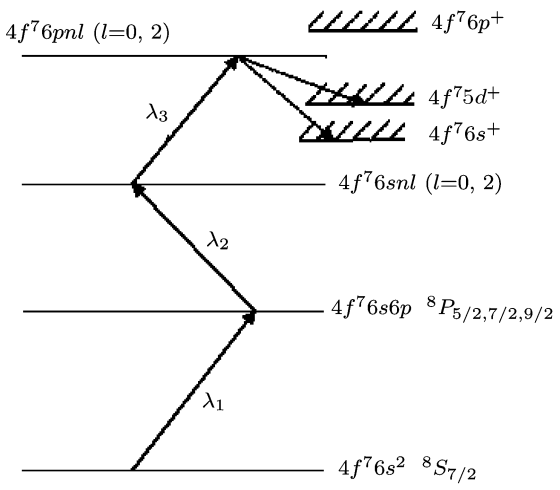


Fig.2. Diagram for the ICE scheme of Eu atom in the experiment. To carry out the autoionization detection, the wavelength of the first laser is fixed at the $4f^7 6s^2 \rightarrow 4f^7 6s6p$ resonance transition, and that of the third laser is fixed near the resonance line of $4f^7 6s^+ \rightarrow 4f^7 6p^+$, while that of the second laser is scanned to excite the atoms to the $4f^7 6snl$ (l=0, 2) Rydberg states.

Scheme I:

$$6s^2\ ^8S_{7/2} \xrightarrow{\lambda_1=459.39\ \text{nm}} 6s6p\ ^8P_{9/2} \xrightarrow{\lambda_2} 6snl\ (l=0,2) \xrightarrow{\lambda_3} 6pnl\ (l=0,2); \quad (1)$$

Scheme II:

$$6s^2\ ^8S_{7/2} \xrightarrow{\lambda_1=462.71\ \text{nm}} 6s6p\ ^8P_{7/2} \xrightarrow{\lambda_2} 6snl\ (l=0,2) \xrightarrow{\lambda_3} 6pnl\ (l=0,2); \quad (2)$$

Scheme III:

$$6s^2\ ^8S_{7/2} \xrightarrow{\lambda_1=466.18\ \text{nm}} 6s6p\ ^8P_{5/2} \xrightarrow{\lambda_2} 6snl\ (l=0,2) \xrightarrow{\lambda_3} 6pnl\ (l=0,2). \quad (3)$$

The three different intermediate states, $4f^7 6s6p\ ^8P_{5/2,7/2,9/2}$, are used for the ICE scheme to study the spectra of Rydberg states of the Eu atom, combined with the autoionization detection. In the experiment, the wavelengths of the first and third lasers are set to one of the intermediate states and to the transition $6s^+ \rightarrow 6p^+_{1/2}$, respectively, while the wavelength of the second laser is scanned.

As the Eu atom has a half-filled $4f$ sub-shell inside the $6s$ shell, the spectrum of Rydberg states of the Eu atom is expected to be much more complicated than the spectrum of ordinary two-electron atoms. Its energy structures may involve a greater number of excitation channels, either from the Rydberg states or the valence states. Alternatively, the main signal from the autoionization detection may be also confused by various disturbing signals, which are from the direct photoionization process, either the one-color stepwise or two-color stepwise process. Therefore, it is essential for us to confirm that all the peaks in the spectrum not only do rely on all dye lasers but also come uniquely from the autoionization detection. Namely, several experimental parameters, the time delay between different laser pulses, the laser intensity, wavelength of lasers, and polarization of the lasers, must be controlled to obtain the signal from the unique excitation route. For instance, to ensure the excitation sequence, the second and third laser pulses are delayed by 8-10 ns and 16-20 ns respectively with respect to that of the first laser; to reduce the possible errors of the experimental data, some efforts have to be made: (a) measure each spectrum several times and take the average of them to reduce the random errors; (b) record the spectrum of an F-P etalon for

correcting the non-linearity in wavelength of the scanning dye laser; (c) calibrate the laser wavelength with the reference lines of a hollow cathode lamp. The uncertainty of wavelength in the present experiment is estimated as ± 0.10 cm^{-1}.

3. Results and discussion

In order to confirm the feasibility of the autoionization detection method, and to choose the most appropriate wavelength of the third laser, it is necessary to investigate the autoionization spectra of the $4f^7 6pnl$ (l=0, 2) states, relevant to the corresponding Rydberg states to be detected. An example of the many observed autoionization spectra is shown in Fig.3, for the detection of the $4f^7 6s8s\ ^6S_{5/2}$ Rydberg state. It is obtained by scanning the wavelength of the third laser from 428.5 nm to 455.5 nm across the core resonance transition $4f^7 6s^+\ J$=3 or $4 \rightarrow 4f^7 6p^+\ J$=3, while the wavelengths of the first two lasers are set to populate the given Rydberg state.

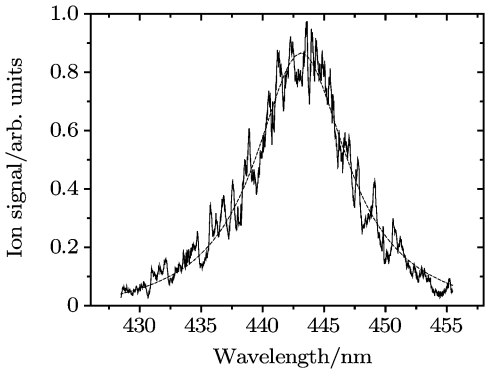


Fig.3. The observed spectrum from the autoionization detection of the $4f^7 6s8s\ ^6S_{5/2}$ Rydberg state. It is obtained by fixing the λ_1 and λ_2 at 466.18 nm and 571.60 nm, respectively, to populate the $4f^7 6s8s\ ^6S_{5/2}$ Rydberg state, while that of the third laser λ_3 is scanned from 428.5 nm to 455.5 nm to cross the core transition $4f^7 6s^+ \rightarrow 4f^7 6p^+$.

Since the spectrum is obtained with the ICE scheme, its profile can be simplified as a standard Lorentz type. Therefore, the experimental values of peak positions and widths of autoionizing states may be obtained by fitting the data to a single Lorentzian profile. In other words, the values of peak position and width of the $6p^+_{1/2}$ autoionizing state of the Eu atom are determined by the Lorentzian profile with a peak at $\lambda_3 = 443.14$ nm, and a width of 9.15 nm, respectively. The uncertainty of the peak position and width by fitting the Lorentzian profile, instead of the Fano profile, is less than the previously mentioned experimental uncertainty (± 0.10 cm^{-1}). As the value of the peak position has been determined at $\lambda_3 = 443.14$ nm, which across the core resonance transition $4f^7 6s^+\ J = 3 \rightarrow 4f^7 6p^+\ J = 3$, the ionization limit ($T_0$) in this work is determined at $4f^7 6s^7 S_3$ ($T_0 = 47404.11$ cm^{-1}).

Obviously, the efficiency of autoionization detection should be proportional to the total cross section of autoionization, whose peak matches the wavelength corresponding to the maximum of detection efficiency. Thus, an ideal detection efficiency may be obtained by adjusting the wavelength of detecting laser near the resonance peak. On the other hand, a large width of the autoionizing state enables us to conveniently adjust the wavelength of the laser λ_3 as it is not so sensitive.

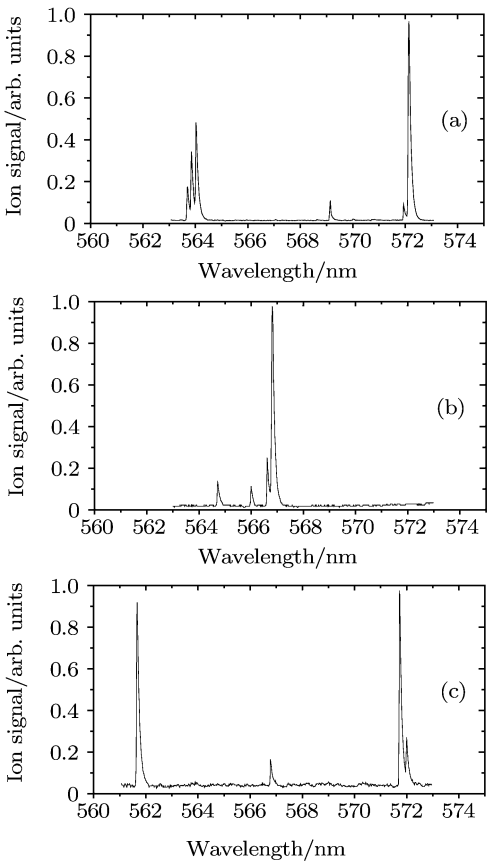


Fig.4. The comparison of spectra of Eu $4f^7 6snl$ Rydberg states obtained with different excitation schemes. They are obtained by fixing λ_1 at (a) 459.39 nm (b) 462.71 nm (c) 466.18 nm, respectively. The λ_3 is fixed at 443.14 nm while the λ_2 is scanned from 563 to 573 nm in the case of (a) and (b), and from 561 to 573 nm in (c).

Armed with the ICE scheme and the autoionization detection described above, we are able to detect the Rydberg states in any given region. Parts of the

spectra of Rydberg states with odd-parity are shown in Fig.4 as examples of such observations. When the wavelength of the third laser is fixed at 443.14 nm, and that of the second laser λ_2 is scanned, the Rydberg states in the region from 38900 cm^{-1} to 39500 cm^{-1} can be detected.

For a given peak in the spectra shown, its photon energy E_2, corresponding to the wavelength of second laser λ_2 of the peak, yields the energy of high-lying states by the relation $E = E_1 + E_2$, where E_1 is the photon energy of the first laser used in the three-color stepwise process. According to the selection rules the possible J values of the peaks can be assigned for the three different excitation schemes mentioned earlier.

In order to make sure that every peak does rely on all the three-color photons, the signals on the oscilloscope have to be examined. Namely, if the ionization signal disappears by blocking any one of the lasers, it is confirmed to come from the three-color stepwise autoionization detection process. With this method one may detect many Rydberg states using different excitation schemes I-III. The results, as listed in Tables 1–3, include the information about the level energy and relative intensity, while the symbols w, m and s represent the three ranges of relative intensity: from 0 to 0.4, 0.4 to 0.7, and 0.7 to 1, respectively.

Table 1. The level energies, relative intensities, and the possible J values of odd-parity Rydberg states obtained using excitation scheme I. The possible J values of these states are determined as 7/2, 9/2 or 11/2, according to the selection rules. The typical experimental uncertainties are estimated to be less than ± 0.10 cm^{-1}, the relative intensities are normalized and classified into three ranges: 0–0.4, 0.4–0.7, and 0.7–1, marked by the symbols w, m and s, respectively.

serial number	λ_2/nm	energy/cm^{-1}	angular momentum/J	intensity
1	563.68	39496.64	7/2	w
2	563.84	39491.61	9/2	w
3	564.00	39486.55	11/2	m
4	568.93	39332.73	11/2	w
5#	571.68	39248.56	7/2, 9/2, 11/2	w
6	571.87	39242.62	7/2	s
7#	615.84	37994.29	7/2, 9/2, 11/2	s
8#	640.15	37377.89	7/2, 9/2, 11/2	s
9#	644.00	37284.87	7/2, 9/2, 11/2	w
10#	647.04	37211.60	7/2, 9/2, 11/2	w

newly discovered.

Table 1 contains the spectral data for the 10 transitions obtained with excitation scheme I. Comparisons with the data in the literature[19] indicate that 5 states in Table 1 are newly discovered. Our data show consistency within the uncertainties with them, where the experiment was carried out with a two-step photoexcitation and photoionization method. According to the selection rules of the transition where the Eu atom in $4f^7 6s^2\ ^8S_{7/2}$ ($J = 0$) state is excited via the intermediate state $4f^7 6s6p\ ^8P_{9/2}$ to Rydberg states, the possible J value of the Rydberg states can be 7/2, 9/2, or 11/2. The results shown in Table 2, give the information about the Rydberg states with the scheme II.

Similarly, the 9 Rydberg atomic states with $4f^7 6snl$ (l=0, 2) configurations excited from the same $4f^7 6s6p\ ^8P_{7/2}$ state are obtained, as listed in Table 2 There are 5 states which are marked with the sign "#" are newly discovered, compared with the data in the literature.[19] According to the selection rules of the transition where the Eu atom in $4f^7 6s^2\ ^8S_{7/2}$ ($J = 0$) state is excited via the intermediate state $4f^7 6s6p\ ^8P_{7/2}$ to Rydberg states, the possible J value of the Rydberg states can be 5/2, 7/2, or 9/2. Table 3 shows the spectral data for bound Rydberg states, which belong to the spectra using excitation scheme III.

Table 2. The level energies, relative intensities, and the possible J values of odd-parity Rydberg states obtained using excitation scheme II. The possible J values of these states are determined as 5/2, 7/2 or 9/2 by the selection rules. The typical experimental uncertainties are estimated to be less than ± 0.10 cm^{-1}, and the relative intensities are normalized and classified into three ranges: 0–0.4, 0.4–0.7, and 0.7–1, marked by the symbols w, m and s, respectively.

serial number	λ_2/nm	energy/cm^{-1}	angular momentum/J	intensity
1	564.77	39306.25	9/2	w
2	566.00	39267.73	5/2	w
3#	566.62	39248.61	5/2, 7/2, 9/2	w
4	566.81	39242.61	7/2	s
5#	637.58	37284.87	5/2, 7/2, 9/2	s
6#	640.57	37211.60	5/2, 7/2, 9/2	w
7	641.22	37195.86	9/2	w
8#	642.81	37157.27	5/2, 7/2, 9/2	m
9#	686.41	36169.35	5/2, 7/2, 9/2	m

newly discovered.

Table 3. The level energies, relative intensities, and the possible J values of odd-parity new Rydberg states obtained using excitation scheme III. The possible J values of these states are determined as 3/2, 5/2 or 7/2, according to the selection rules. The typical experimental uncertainties are estimated to be less than ± 0.10 cm^{-1}, and the relative intensities are normalized and classified into three ranges: 0–0.4, 0.4–0.7, and 0.7–1, marked by the symbols w, m and s, respectively.

serial number	λ_2/nm	energy/cm^{-1}	angular momentum/J	intensity
1	561.68	39242.63	7/2	s
2#	566.80	39082.28	3/2, 5/2, 7/2	w
3	571.60	38933.85	5/2	s
4#	571.87	38925.91	3/2, 5/2, 7/2	w
5#	594.99	38246.63	3/2, 5/2, 7/2	s
6#	634.04	37211.60	3/2, 5/2, 7/2	s
7#	636.24	37157.27	3/2, 5/2, 7/2	w
8#	637.76	37119.81	3/2, 5/2, 7/2	w
9	682.23	36097.79	7/2	w
10	683.40	36072.91	5/2	w
11	684.67	36045.75	3/2	m

newly discovered.

Table 3 contains the spectral data for the 11 transitions obtained with excitation scheme III. Comparisons with the data in the literature[19] indicate that 6 states in Table 3 are newly discovered. According to the selection rules of the transition where the Eu atom in $4f^7 6s^2\ ^8S_{7/2}$ ($J = 0$) state is excited via the intermediate state $4f^7 6s6p\ ^8P_{5/2}$ to Rydberg states, the possible J value of the Rydberg states can be 3/2, 5/2, or 7/2. Similarly, the results shown in Table 3 give the information about the Rydberg states with the scheme III.

Compared with the values in previous studies, 11 new Rydberg states in the same energy region is obtained; our data show a good agreement within the uncertainties with them, where the experiment was carried out with a two-step photoexcitation and photoionization method. Two possible reasons can explain why they could not be found in the previous photoionization experiment: firstly, the states shown in Tables 1–3 cannot be accessible if one uses the excitation schemes there. Secondly, unlike the previous experiment carried out with a two-step photoexcitation and photoionization method, a three-step autoionization detection method is employed here. Apparently all the states tabulated in Tables 1–3 are odd parity according to the atomic transition law of parity. In this work, we not only obtain some experimental values, such as the peak positions, but also make some efforts on the relative intensities of the states which cannot be found in previous works, and

the angular momentum of the states, according to the selection rules: $\Delta J = 0, \pm 1 (0 \nrightarrow 0)$. For instance, the angular momentum of No.1 in Table 2 atomic state is determined as 9/2, compared with the data in the literature,[19] while the possible value should be 5/2, 7/2 or 9/2 according to the quantum theory for the excitation scheme II.

Furthermore, some efforts also have been made on the effective principal quantum number of these states. As we know, the effective principal quantum number n^* is obtained from the Rydberg–Ritz formula as (where n is not the necessary principal quantum number, but an integer close to n^*)

$$n^* = \sqrt{\frac{R_{\mathrm{Eu}}}{T_0 - E_{\mathrm{Ryd}}}}, \tag{4}$$

where R_{Eu} is the mass corrected Rydberg constant for Eu I (R_{Eu}=109736.92 cm^{-1}), E_{Ryd} is the energy of the Rydberg level obtained experimentally. The ionization limit T_0 is given by

$$T_0 = I_{\mathrm{P}} + E_{\mathrm{ion}}, \tag{5}$$

where I_{P} is the first ionization potential and E_{ion} is the energy of the ionic level at which the series is converging. In this work, as we stated above, the value of T_0=47404.11 cm^{-1}for $4f^7 6s\ ^7S_3$ series limit.

Table 4 lists the possible J value and the effective principal quantum number of the bound Rydberg states of Eu I which is obtained by fitting Rydberg–Ritz formula.

Table 4. Energy levels, angular momentum, and effective principal quantum number of the Rydberg states obtained in this work.

energy/cm^{-1}	excitation scheme	angular momentum/J	effective principal quantum number
39496.64	I	7/2	3.725
39491.61	I	9/2	3.724
39486.55	I	11/2	3.723
39332.73	I	11/2	3.687
39306.25	II	9/2	3.681
39267.73	II	5/2	3.672
39248.56#	I, II	7/2, 9/2	3.668
39242.62	I, II, III	7/2	3.667
39082.28#	III	3/2, 5/2, 7/2	3.631
38933.85	III	5/2	3.599
38925.91#	III	3/2, 5/2, 7/2	3.598
38246.63#	III	3/2, 5/2, 7/2	3.462
37994.29#	I	7/2, 9/2, 11/2	3.415
37377.89#	I	7/2, 9/2, 11/2	3.308
37284.87#	I, II	7/2, 9 /2	3.293
37211.60#	I, II, III	7/2	3.281
37195.86	II	9/2	3.279
37157.27#	II, III	5/2, 7/2	3.273
37119.81#	III	3/2, 5/2, 7/2	3.267
36169.35#	II	5/2, 7/2, 9/2	3.125
36097.97	III	7/2	3.115
36073.01	III	5/2	3.112
36045.73	III	3/2	3.108

newly discovered.

Examinations of the present work show that 11 states in the region from 38900 cm^{-1} to 39500 cm^{-1} and from 38900 cm^{-1} to 39500 cm^{-1} using three different excitation schemes, marked with the sign "#",

have not been reported previously. It is important to point out that although the energy regions have been studied in the literature, with different excitation paths and different detection methods from ours, the results are expected to be different. Apart from the new Rydberg states, the effective principal quantum number of the bound Rydberg states, which have not been reported in the literature, are obtained by fitting Rydberg–Ritz formula to the experimental data. In addition, the possible J values of the states which are not marked with "#" are determined by comparing with the data in Ref.[19], such as we stated above. Similarly according to the selection rules: $\Delta J = 0, \pm 1 (0 \not\rightarrow 0)$, comparisons between the data in Tables 1–3 are also very meaningful. For instance, the state at 37211.60 cm^{-1}, the possible angular momentum is $J = 7/2$, $9/2$, $11/2$ from the excitation scheme I while it is $J = 5/2$, $7/2$, $9/2$ from the excitation scheme II, and it is $J = 3/2$, $5/2$, $7/2$ from the excitation scheme III. Therefore, the comparison between the three excitation schemes indicates that angular momentum of the state should be $7/2$. Through the comparison between the three different excitation schemes, the angular momentum of these states are obtained.

It is worth while to point out that our observations cover the energy ranges using autoionization detection and the ICE scheme have not been reported previously.

4. Conclusions

In this paper, isolated-core excitation and three-color three-step resonance ionization spectroscopy are first combined to study the spectra of Rydberg states of Eu atom. The autoionization detection method with three different excitation paths via $4f^7 6s6p[^8P_{5/2}]$, $4f^7 6s6p[^8P_{7/2}]$ and $4f^7 6s6p[^8P_{9/2}]$ have been used to measure the high-lying Rydberg states with odd parity. In this work, the spectra of bound Rydberg states of Eu atom with odd-parity are reported, which cover the energy regions from 36000 cm^{-1} to 38250 cm^{-1} and from 38900 cm^{-1} to 39500 cm^{-1}. The study provides the information about level energies, the relative line intensity and the possible J values and obtains the effective principal quantum number n^* of the high-lying states. This work not only confirms the results of many states studied in the related reference papers, but also discovers 11 new Rydberg states of Eu atom. This will enrich our knowledge on the Eu atomic spectroscopy, and stimulate further theoretical efforts on improving applications of the quantum theory on the complex atomic systems.

References

[1] Paspalakis E, Kylstra N J and Knight P L 1999 *Phys. Rev.* A **60** 642
[2] Lyras A and Bauchau H 1999 *Phys. Rev.* A **60** 4781
[3] Harris S E 1989 *Phys. Rev. Lett.* **62** 1033
[4] Bhattacharyya S, Razvi M A N, Cohen S and Nakhate S G 2007 *Phys. Rev.* A **76** 012502
[5] Ogawa Y and Kujirai O 1999 *J. Phys. Soc. Jpn.* **68** 428
[6] Bhattacharyya S, Nakhate S G, Jayasekharan T and Razvi M A N 2006 *Phys. Rev.* A **73** 062506
[7] Schniepp H and Sandoghdar V 2002 *Phys. Rev. Lett.* **89** 257403
[8] Yi J H, Lee J and Kong H J 1995 *Phys. Rev.* A **51** 3053
[9] Bi'emont E, Garnir H P, Li Z S, Lokhnygin V, Palmeri P, Quinet P, Svanberg S, Wyart J F and Zhang Z G 2001 *J. Phys.* B **34** 1869
[10] Nakhate S G, Razvi M A N, Connerade J P and Ahmad S A 2000 *J. Phys.* B: *At. Mol. Opt. Phys.* **33** 5191
[11] Bhattacharyya S, D'Souza R, Rao Pushpa M and Razvi M A N 2003 *Spectrochimica Acta* Part B **58** 469
[12] Li S B and Dai C J 2003 *J. Quant. Spectrosc. Radiat. Transfer* **77** 345
[13] Zhang Y, Dai C J and Li S B 2004 *J. Electron Spectrosc. Relat. Phenom.* **135** 63
[14] Li S B, Dai C J, Sun W and Xue P 2001 *J. Phys.* B: *At. Mol. Opt. Phys.* **34** 2123
[15] Li S B and Dai C J 2007 *Chin. Phys.* **16** 382
[16] Lu J, Dai C J, Xu Y F and Li S B 2001 *Chin. Phys. Lett.* **18** 1192
[17] Dai C J and Zhao X A 1995 *J. Quant. Spectrosc. Radiat. Transfer* **54** 1019
[18] Lu J, Dai C J, Li C Q, Xu X H, Liu Z D and Tang J C 1999 *J. Quant. Spectrosc. Radiat. Transfer* **61** 339
[19] Martins M, Godehusen K, Gerth Ch, Zimmermann P, Schulz J, Wernet Ph and Sonntag B 2002 *Phys. Rev.* A **65** 030701